The Effects of El Niño-South Oscillation on the Winter Haze Pollution of China

Shuyun Zhao[1,2], Hua Zhang[1,2], Bing Xie[1,2]

[1]Laboratory for Climate Studies, National Climate Center, China Meteorological Administration, Beijing, China

[2]Collaborative Innovation Center on Forecast and Evaluation of Meteorological Disasters, Nanjing University of Information Science & Technology, Nanjing, China

Correspondence to: Hua Zhang (huazhang@cma.cn)

Abstract. It is reported in previous studies that El Niño-South Oscillation (ENSO) influences not only the summer monsoon, but also the winter monsoon over East Asia. This contains some clues that ENSO may affect the winter haze pollution of China, which has become a serious problem in recent decades, through influencing the winter climate of East Asia. In this work, we explore the effects of ENSO on the winter (from December to February) haze pollution of China statistically and numerically. Statistical results reveal that the haze days of southern China tend to be less (more) than normal in El Niño (La Niña) winter; whereas the relationships between the winter haze days of northern and eastern China and ENSO are not significant. Results from numerical simulations also show that ENSO influences the winter atmospheric contents of anthropogenic aerosols over southern China more obviously than it does over northern and eastern China. Under the emission level of aerosols for the year 2010, the winter atmospheric contents of anthropogenic aerosols over southern China are generally more (less) than normal in El Niño (La Niña) winter. It is because that the transports of aerosols from South and Southeast Asia to southern China are enhanced (weakened), which mask the better (worse) scavenging conditions for aerosols in El Niño (La Niña) winter. The frequency distribution of the simulated daily surface concentrations of aerosols over southern China indicates that the region tends to have less clean and moderate (heavy) haze days, but more heavy (moderate) haze days in El Niño (La Niña) winter.

1 Introduction

Haze pollution, especially in winter, has become a very serious problem for China in recent decades (Ding and Liu, 2014; Tao et al., 2016). For example, in January 2013, most parts of central and eastern China experienced an extremely heavy and persistent haze pollution (Tao et al., 2014; Mu and Zhang, 2014; Zhang et al., 2014; Wang et al., 2014a; b; Zou et al., 2017).

In the last decade, haze pollution in winter has received wide concerns from the scientific community, the government of China, and the public.

Haze pollution is a phenomenon mainly caused by human-emitted pollutants under stagnant meteorological conditions. Increasing anthropogenic emissions of aerosols and their precursors in recent decades are the main reasons for the worsening air qualities in China (Cao et al., 2007; Zhang et al., 2012; Zhu et al., 2012). In addition to the increase in anthropogenic emissions of aerosols and their precursors, climate changes caused by anthropogenic and/or natural forcings also exert great influences on the haze pollution in China, especially through changing the strength of East Asian Monsoon (Zhang et al., 2010; 2014; Liu et al., 2011; Yan et al., 2011; Chin, 2012; Zhu et al., 2012; Mu and Zhang, 2014; Chen and Wang, 2015; Li et al., 2016a; b; Cai et al., 2017). Studies generally showed that the wintertime haze days across central and eastern China had a close negative relationship with the strength of East Asian Winter Monsoon (EAWM) (Zhang et al., 2014; Mu and Zhang, 2014; Chen and Wang et al., 2015; Li et al., 2016a; Cai et al., 2017). In summer, the increase in surface aerosol concentration and optical depth over eastern and northern China always correlates with the weakening of the East Asian Summer Monsoon (EASM) (Zhang et al., 2010; Yan et al., 2011; Zhu et al., 2012). Whereas Yang et al. (2014) found that the gaseous pollutant of surface O_3 over China had a positive relationship with the EASM.

Wang et al. (2015) and Zou et al. (2017) revealed that the increasing winter haze pollution in eastern China in recent years was related to the decreasing Arctic sea ice in preceding autumn. Many studies suggested that under global warming, the future climate would be more stagnant and the weather conditions conducive to severe haze in eastern China would be more frequent (Jacob and Winner, 2009; Wang et al., 2015; Cai et al., 2017). But Jacob and Winner (2009) also pointed out that the effects of future climate change on particulate matter (PM) were complicated, as the projection of precipitation, wildfires, atmospheric chemistry, and natural emissions of aerosols by models were still in need of improvement.

ENSO is the dominant changing mode of the tropical sea surface temperature (SST) on interannual scale (Rasmusson and Carpenter, 1982), of which the climatic effects are global (Bjerknes, 1972; Huang and Wu, 1989; Zhang et al., 1999; Lau and Nath, 2003; Zhai et al., 2016, etc.). ENSO not only influences the EASM (Chang et al., 2000; Li et al., 2007; Zhao et al., 2017, etc.), but also influences the EAWM, especially over low latitudes (Chen et al., 2013; He and Wang, 2013; Kim et al., 2016, etc.), which means that ENSO may affect the haze pollution over East Asia through its influences on the monsoon circulation.

Wu et al. (2013) found that the aerosol variations over the Maritime Continent and western North Pacific presented a biennial feature, which could be attributed to the impacts of ENSO. From the results of Wu et al. (2013), it seemed that ENSO only influenced the aerosols over eastern China (30°–40°N, 110°–120°E) around October of El Niño or La Niña developing years and July of El Niño or La Niña decaying years. Gao and Li (2015) revealed statistically that El Niño (La Niña) events were more likely to bring more (less) haze days in eastern China (25°–35°N, 105°–122.5°E). Feng et al. (2016) simulated the influences of the 1994/1995 El Niño Modoki event on the aerosol concentrations over southern China (20°–35°N, 105°–120°E), and found that the aerosol concentrations increased during the mature phase (in boreal winter) of the event. Feng et al. (2017) simulated the influences of the 1998/1999 and 2000/2001 La Niña Modoki events on the aerosol concentrations over eastern China (105°–120°E), and found that the geographical distributions of aerosols over eastern China during the winters of the two events were opposite with each other. Most previous studies discussed the effects of ENSO on the winter haze pollution of China based on observation or case simulation separately. In this study, we try to explore the effects of ENSO on the winter haze pollution of China statistically and numerically. ENSO is a recurring climate pattern, and many climate centers of the world monitor it systematically and use it in climate prediction extensively. Therefore, exploring the effects of ENSO on the winter haze pollution in China may provide useful information in the prediction of haze for the country.

The article is organized as follows: methodology is given in section 2, including data and model introduction; results including statistical and model results, are presented in section 3, followed by conclusions and discussions in section 4.

2 Methodology

2.1 Data used in statistical analysis

We firstly analyze the relationship between the winter haze days of China and global SST in section 3. The monthly haze days from the data set for haze project version 1.0 of the National Meteorological Information Center, China Meteorological Administration (CMA) are used. The CMA defines haze using visibility (<10 km) and relative humidity (<80%) (Tao et al., 2014). The time-span of the data set is January 1954~July 2014, but only the data after 1960 are actually used in this study, as the data set has steadily included more than 2000 stations since 1960. A merged monthly SST data (Hurrell, et al., 2008) formed by the SST data of the Hadley Centre and the National Oceanic and Atmospheric Administration (NOAA) is used in the correlation analysis. The SST data together with a merged sea ice (SI) data of the same sources are used in the following

numerical simulation. The SST and SI data are both from 1870 to 2012, with a horizontal resolution of 1°×1°.

2.2 Model description and experimental set-up

The aerosol-climate coupled model BCC_AGCM2.0_CUACE/Aero (Zhang et al., 2012) of the National Climate Center (NCC), CMA, is used in the numerical study of the effects of ENSO on the atmospheric contents of aerosols. The coupled model composes of the NCC/CMA climate model (BCC_AGCM2.0, Wu et al., 2010) and the CMA Unified Atmospheric Chemistry Environment/Aerosol model (CUACE/Aero, Gong et al., 2002, 2003). The coupled model employs a horizontal T42 spectral resolution (about 2.8°×2.8°) and a hybrid vertical coordinate with 26 levels, the top of which is located at about 2.9 hPa. Five types of aerosols (including their emissions, gaseous chemistry, transports, coagulations, and removals): sulfate (SF), black carbon (BC), organic carbon (OC), dust, and sea salt are considered in the model. The emissions of the first three types of aerosols and/or their precursors are prescribed, and the last two types of aerosols are emitted online (Gong et al., 2002). The particle radii of each type of aerosol are divided into 12 size bins from 0.005 to 20.48 μm. All types of aerosols are assumed to be externally mixed with each other. Sulfate, organic carbon, and sea salt are assumed to be hygroscopic, and the other two types of aerosols are assumed to be non-hygroscopic. The coupled model has been introduced, evaluated, and used in many studies of the radiative forcing and climatic effects of aerosols (e.g., Wang et al., 2015; Zhao et al., 2014; Zhang et al., 2016).

Three groups of experiments are conducted (Table 1), named CLI, EL, and LA, with each group including 20 members by altering initial conditions. To get different initial conditions, a preparation experiment is run firstly with the model's default setting (Zhao et al., 2014). Three types of files (initial, restart, and history files) of the preparation experiment are output, and the output frequency is set to daily. 20 initial files output from the preparation experiment are then used as the different initial conditions for different ensemble members. The group of CLI uses the climatological-mean (from 1981 to 2010) monthly SST and SI, which have been introduced in the section 2.1 but interpolated to the model's resolution, as boundary conditions. In the groups of EL and LA, the climatological-mean monthly SST is superposed by El Niño and La Niña SST perturbations, respectively, and the SI is identical to that in CLI. The El Niño and La Niña SST perturbations are obtained by scaling a typical ENSO mode (Figure 1a) with the average monthly Niño3.4 indices of 21 El Niño and 18 La Niña events (selected from 1951 to 2015, Figure 1b), respectively. The Niño3.4 indices from January 1951 to date can be downloaded from the website of NCC/CMA (cmdp.ncc-cma.net/download/Monitoring/Index/M_Oce_Er.txt). The typical ENSO mode is obtained through the

regression between the monthly Niño3.4 index and the SST field after removing their linear trends. The running period of the group of CLI is from October to the next August, to testify if the model can capture the general features of the circulations of the East Asian winter and summer monsoons. In the testifying process, the geopotential height and wind from the National Centers for Environmental Prediction (NCEP) reanalysis data are used. Whereas the running periods of EL and LA are both from October to the next February. The results in boreal winter (December, January, and February, or DJF for short) of the three groups are used in analysis, allowing prior two months for the atmosphere to response to SST perturbations.

The emission data of SF, BC, OC, and/or their precursors used in all experiments are from the Representative Concentration Pathway 4.5 (RCP 4.5) of the Intergovernmental Panel on Climate Change (IPCC) for the year of 2010. In this study, only the changes in the atmospheric contents of SF, BC, and OC caused by different SST perturbations are analyzed, as the three types of aerosols are mainly emitted by anthropogenic activities and important components of haze pollutants. In the analyzing process, the median instead of the average of the changes of a specific variable between different groups of experiments (e.g., EL – CLI) is used, as median is more robust and resistant to extreme large or small values that may happen in some ensemble members. And we also mark the grids where the differences of a specific variable between more than 70% pairs of ensemble members have the same sign with the median differences, as a reflection of significance.

3 Results

3.1 Statistical results

In this section, we firstly present the geographical distribution of the winter haze days in mainland China over the past about 50 years and since 2000. Then, three typical polluted regions are selected, and the correlations between their respective winter haze days and global SST are analyzed.

It's seen from Figure 2a that Beijing, the southwest part of Hebei, the central and south parts of Shanxi, the central part of Shaanxi, and the north part of Henan suffered winter haze pollution more frequently than elsewhere in China during 1960−2013, with the largest value of DJF mean monthly haze days among 10~20. The diffusive conditions of these areas are not good because of the influences of the Tai-hang and Qin-ling mountains. Besides the above areas, stations with more than 5~10 DJF mean monthly haze days during 1960−2013 distributed densely in the provinces of Hubei, Hunan, Jiangxi, Zhejiang, Guangxi and Guangdong. Compared with 1960−2013, winter haze pollution in mainland China generally became more

frequent during 2000−2013 (Figure 2b). For example, in the Yangtze River Delta and Pearl River Delta, stations with 5~10 and 10~20 DJF mean monthly haze days during 2000−2013 were much more than that during 1960−2013. At some stations of Shanxi province, the DJF mean monthly haze days during 2000−2013 were even more than 20 (Figure 2b). The locations of the Chinese provinces mentioned above and in the following, can be found in Figure S1in the supplementary document.

Three representative regions: JJJ (Beijing, Tianjin, and Hebei province; accounting for 179 stations), JZH (Jiangsu and Zhejiang provinces, and Shanghai; accounting for 164 stations), and GG (Guangdong and Guangxi provinces; accounting for 178 stations) are selected to represent northern, eastern, and southern China, respectively. It is seen from Figure 3 that the DJF mean monthly haze days of these three regions were generally less than 3 before the year of 2000, with a small peak around 1980 in northern and eastern China. After the year of 2000, the DJF mean monthly haze days over eastern and southern China grew rapidly. The DJF mean monthly haze days of northern China increased much later than the other two regions after the year of 2000. Actually, the DJF mean monthly haze days over northern China were relatively few until 2012, which was consistent with the result of Chen and Wang (2015).

Considering that the increases in the DJF mean monthly haze days over eastern and southern China increased too abruptly after the year of 2010, only the winter haze days of the three regions from 1960 to 2010 are used in analyzing their relationships with winter SST. In order to remove the inter-decadal variabilities, we applied a 2-8 years band-pass filtering to both the data of haze days and SST. It is seen from Figure 4 that only the winter haze days of southern China have significant negative relationships with the equatorial SST over central and eastern Pacific and central Indian Ocean, and positive relationships with the equatorial SST over western Pacific. The geographical distribution of the correlation coefficients between the winter haze days over southern China and SST is generally an opposite phase of the typical ENSO mode shown in Figure 1a, indicating that southern China tends to suffer more (less) haze days than normal in La Niña (El Niño) winter. This can also be seen from the comparison of the DJF mean monthly haze days between several selected pairs of La Niña and El Niño winters over southern China (Figure S2). In order to avoid the influences of the emission variations of haze particles and their precursors, each pair of La Niña and El Niño winters are selected with their interval not longer than 2 years.

The relationships between the winter haze days of northern and eastern China and equatorial SST are not significant (Figures 4a and 4b), indicating that ENSO does not influence the winter haze days of these two regions significantly. It's probably

because that as a tropical phenomenon, ENSO affects the climate over southern China more directly than that over northern and eastern China, especially in winter when the Western Pacific Subtropical High (WPSH) is generally weaker and located more south than other seasons. Zou et al. (2017) linked the extreme winter haze events over East China Plains (112°–122°E, 30°–41°N, including JJJ and most parts of JZH) to Arctic sea ice loss in the preceding autumn and extensive Eurasia snow fall in early winter. Gao and Li (2015) found that the winter haze days of eastern China had positive relationship with the SST over eastern equatorial Pacific. But the "eastern China" in Gao and Li (2015) included most regions between the Yangtze and Yellow rivers east of 105°E, which was much larger and more west than the representative region of eastern China in this work, and more south and west than the concerned region in Zou et al. (2017).

3.2 Model results

3.2.1 Winter and summer circulations, and the atmospheric contents of aerosols

First of all, the simulated winter and summer circulations over East Asia in the group of CLI are testified by comparing with NCEP reanalysis data (Figure 5). The model can capture the general features of the winter and summer circulations over East Asia. For example, in winter, the deepening of East Asian Trough (EAT), the overwhelming of northwesterly over the east part of China, and the strengthening of the easterly north of the equator are all depicted by model results (Figure 5a); In summer, the northward shift of WPSH, and the strengthening of the cross-equatorial westerly over the Indian Ocean and Maritime Continent are generally captured by the model (Figure 5b). But the simulated EAT in winter by the model is weaker and narrower, and locates more west than NCEP reanalysis data. In summer, the simulated WPSH is weaker and locates more east than NCEP reanalysis data. It seems that the simulated cross-equatorial flow is stronger than reanalysis data both in winter and summer, which is probably the reason for the weakness of the simulated EAT in winter and WPSH in summer. In the model results of the group of CLI, the stronger cross-equatorial westerly over the Indian Ocean and Maritime Continent obstructs the westward stretch of the WPSH in summer, resulting in positive precipitation biases over South Asia and Southeast Asia, and negative precipitation biases over southern China (Zhao et al., 2014).

The simulated winter surface concentrations (CONCsur) of aerosols and aerosol loadings in the group of CLI (Figure 6) show that central and eastern China (about east of 105°E) are the most haze polluted regions of the country, in line with the observational distribution of winter haze days shown in Figure 2. The maximum of the winter CONCsur of aerosols centers in

Henan province, and is about 20 μg m^{-3}. Comparing with other observational studies (e.g., Cao et al., 2007; Zhang and Cao, 2015; Cai et al., 2017), the simulated CONCsur of aerosols shown in Figure 6a are underestimated by about 1~2 orders of magnitude. It should be illustrated that the aerosol CONCsur in this study are the aerosol concentrations at the lowest level of the model. As has been introduced in section 2.2, the model used in this study has 26 levels in the vertical hybrid σ-pressure axis, and the mid height of the lowest level is about 50 ~ 70 meters above the surface in China (not shown). Therefore, the aerosol concentrations at the lowest level of the model actually reflect the mean of the aerosol concentrations from the surface to a height of about 100 ~ 140 meters (or maybe even higher) above the surface. This certainly brings about underestimations as to aerosol CONCsur. Another reason for the underestimation is that we exclude all nature-emitted aerosols, in order to focus our attentions on haze, as another meteorological disaster occurring frequently in late winter and spring over northern China – sandstorm – has quite different weather conditions with haze. The exclusion of nature-emitted aerosols (mainly dust aerosol) is also the reason why the northwestern China is much cleaner than it is expected to be.

The maximum of the simulated winter aerosol loadings in China is 21 ~ 25 mg m^{-2}, and heavy aerosol loadings (≥18 mg m^{-2}) in China locate east of 105°E, and between the Yellow and Yangtze rivers (Figure 6b). The median of 10 models that participated in the Aerosol Comparisons between Observations and Models (AeroCom, http://aerocom.met.no/cgi-bin/aerocom/surfobs_annualrs.pl) showed that the maximums of the loadings of SF, BC, and OC in January 2000 in China were 15 ~ 30, 2.5 ~ 5, and more than 10 mg m^{-2}, respectively. The model used in this study is also a member of AeroCom. Zhao et al. (2014) have compared the simulated loadings of five kinds of aerosols (SF, BC, OC, sea salt, and dust) by the model with AeroCom median, and found that the model generally simulated the distributions and magnitudes of aerosol loadings well, though with some underestimations in BC and OC.

3.2.2 The effects of ENSO on winter circulation and precipitation

The effects of ENSO on the winter circulation and precipitation over East Asia are discussed firstly, as these meteorological fields determine the transports, diffusions, removals, and consequently the atmospheric contents of aerosols.

Two important features are apparent in the winter anomalous circulation field caused by El Niño (Figure 7a). Firstly, negative

and positive anomalous geopotential heights at 500 hPa are seen near Ural Mountains and Lake Baikal, respectively. Secondly, two anomalous anticyclones at 850 hPa are seen over western North Pacific, with one in the Philippine Sea and the other one in the mid latitude. It is expected that the anomalous southwesterly in the northwest of the Philippine Sea anticyclone brings more water vapor and also more aerosols to southern China, as Indo-China Peninsula and South Asia are both areas with heavy aerosol loadings (Figure 6b). Whereas the anomalous geopotential height at 500 hPa caused by La Niña are positive and negative near Ural Mountains and Lake Baikal, respectively, and two anomalous cyclones are caused by La Niña over western North Pacific (Figure 7b).

The differences in circulation between El Niño and La Niña winters are shown in Figure 7c. It is seen in Figure 7c that the negative and positive anomalies in 500 hPa geopotential height caused by El Niño are more obvious than that in Figure 7a over Ural Mountains and Lake Baikal, respectively. And the anomalous anticyclones in the western North Pacific are also more obvious than that in Figure 7a. Wang et al. (2000) found that the anomalous anticyclones over western North Pacific formed in the boreal autumn of a developing El Niño, attained its peak in winter, and persisted into the following spring and early summer. In the sea level pressure field, the land-sea gradient in winter is decreased by El Niño (not shown), indicating that El Niño causes a weakness of the EAWM. The weakness of the EAWM caused by El Niño can also be seen from the weakness of East Asian jet stream and the decrease in EAWM index caused by El Niño (Figure S3). The EAWM index used in Figure S3 is the one defined by Li and Yang (2010). It has been suggested in previous studies that the weakness of East Asian jet stream and the Philippine Sea anticyclonic anomalies in winter caused by El Niño connected with each other by local Hadley circulation over East Asia (Kang and Lee, 2017).

Previous studies have also found that the EAWM tended to be weak in El Niño winter (e.g., Chen et al., 2000; Huang et al., 2012; Wang and Chen, 2014; Kang and Lee, 2017). Wang et al. (2000) has explored how ENSO influenced its upstream climate in East Asia, and found that the Pacific-East Asian teleconnection (PEAT) was the key bridge. PEAT is a vorticity wave pattern that starts from the central Pacific and extends poleward and westward to East Asia. In Figure 7c, PEAT can be recognized from the 850 hPa wind anomalies with a cyclonic vorticity over the central Pacific, the anticyclonic vorticities over western North Pacific, and a cyclonic vorticity over northeast Asia. The PEAT can be seen more clearly from the differences in the stream function at 500 hPa between El Niño and La Niña winters (Figure S4), which has an opposite sign with vorticity.

Corresponding to the anomalous anticyclones at 850 hPa over western North Pacific caused by El Niño, winter precipitation decreases over Indo-China Peninsula and northwestern Pacific, and increases over southern China (Figure 8a). In contrast, precipitation increases over Indo-China Peninsula and northwestern Pacific, and decreases over southern China during La Niña winter (Figure 8b). The opposite effects of El Niño and La Niña on the winter precipitation over southern China can be seen more clearly in Figure 8c, which is in accordance with the observational relationship between ENSO and China precipitation in winter (http://cmdp.ncc-cma.net/pred/cn_enso.php?product=cn_enso_corr&season=DJF#corr). The decrease in winter precipitation over southern China caused by La Niña is very likely the reason for the more-than-normal haze days over the region during La Niña winter (Figure 4c), as less precipitation means slower cleaning particles out of the atmosphere (Figures 10b and 10c), which will be discussed in the next section. Another reason probably cannot be neglected that drier conditions over southern China during La Niña winter can avoid mistaking haze to fog days.

3.2.3 The effects of ENSO on winter atmospheric contents of aerosols

In this section, the changes in the winter aerosol CONCsur and loadings over China caused by ENSO are presented, and then the mechanism how ENSO affects the winter atmospheric contents of aerosols is analyzed from the perspective of wet and dry depositions and interregional transports of aerosols.

It is seen from Figure 9a that the winter CONCsur of aerosols are decreased by El Niño over northeastern China and eastern China. The winter aerosol CONCsur are also decreased by La Niña over northeastern China and eastern China, as well as the north part of northern China and most areas south of the Yangtze river (Figure 9b). Over southern China, although the increases in the winter CONCsur of aerosols caused by El Niño are not very clear in Figure 9a, they are obvious by comparing with La Niña winter (Figure 9c), which is generally in line with the simulation result of Feng et al. (2016). It is found from Figure 9d that the winter aerosol loadings are increased by El Niño over most areas east of 105°E and south of 40°N, and decreased over northeastern China and the north part of northern China. From Figure 9e, it is seen that the anomalous winter aerosol loadings caused by La Niña present a meridional "- + -" pattern over the east part of China. The different influences of El Niño and La Niña on the winter aerosol loadings are the most obvious over the large areas south of the Yangtze river (Figure 9f).

From Figures 9c and 9f, it is found that the differences in the atmospheric contents of aerosols between El Niño and La Niña winters are more obvious over southern China than the other areas of the country. This is to some extent in line with the results

in Figure 4 that only the winter haze days over southern China have significant relationship with ENSO. Therefore, in the following analysis, we focus on the mechanism how ENSO affects the winter atmospheric contents of aerosols over southern China.

It has been discussed in section 3.1 that the haze days over southern China tended to be less (more) than normal in El Niño (La Niña) winter, which is to some extent contradictory to the increase (decrease) in the winter atmospheric contents of aerosols over southern China caused by El Niño (La Niña). In the following of this section, we firstly explore the reasons for the increase (decrease) in the winter atmospheric contents of aerosols caused by El Niño (La Niña) over southern China. Then, we try to explain why the changes in the winter haze days and atmospheric contents of aerosols caused by ENSO over southern China are not consistent with each other.

As the emissions of aerosols are kept the same in all experiments (section 2.2), how quickly aerosols are removed from the atmosphere, especially through wet deposition, can affect the atmospheric contents of aerosols greatly (Zhang et al., 2016). It is found that ENSO influences the winter wet depositions more obviously than the winter dry depositions of aerosols over China (Figure 10). The winter dry depositions of aerosols are decreased both by El Niño and La Niña over southern China (Figures 10c–f). Comparing with dry deposition, wet deposition is a faster process. The winter wet depositions of aerosols over southern China are increased (decreased) by El Niño (La Niña) (Figure 10a–c), corresponding to the changes in winter precipitation (Figure 8). Comparing Figure 9 and 10, it is found that the winter atmospheric contents and wet depositions of aerosols are both increased (decreased) by El Niño (La Niña) over southern China. It seems that the changes in the winter wet depositions of aerosols are the results rather than the reasons of the changes in the winter atmospheric contents of aerosols over southern China.

Besides local emissions and removals, the interregional transports of aerosols can also influence the atmospheric contents of aerosols over a specific region. It was mentioned in Zhang et al. (2016) that South and Southeast Asia had become the important source areas of anthropogenic aerosols in 2010, which was also seen in the simulated aerosol CONCsur and loadings over these regions (Figure 6). A low-level anomalous anticyclone (cyclone) is caused by El Niño (La Niña) over the Philippine Sea in winter (Figure 7). The southwesterly (northeasterly) at the northwest of the anomalous anticyclone (cyclone) leads to an enhanced (weakened) transports of aerosols from South and Southeast Asia to southern China in El Niño (La Niña) winter

(Figure 11). As the changes in the winter atmospheric contents of aerosols over southern China caused by ENSO cannot be explained by local emissions or removals, it seems can only be attributed to the changes in the transports of aerosols from South and Southeast Asia to southern China. Zhu et al. (2012) has also pointed out that in determining aerosol concentrations, the changes in monsoon circulation were more dominant than that in precipitation (or wet deposition of particles) in East Asia. It has been revealed statistically in Figure 4c that southern China tended to suffer more (less) haze days than normal in La Niña (El Niño) winter, which was also seen in the 4 selected pairs of El Niño and La Niña winters (Figure S2) with one of them near 2010 (in numerical simulations, the aerosol emissions are fixed in 2010). However, numerical results show that La Niña (El Niño) causes a decrease (increase) in the winter atmospheric contents of aerosols over southern China (Figure 9). Is it possible for southern China to have more (less) haze days but less (more) atmospheric contents of aerosols than normal in La Niña (El Niño) winter? To answer this question, the frequency distributions of the simulated winter daily aerosol CONCsur averaged over southern China (21°N–27°N, 104°–118°E, see Figure S1) in the groups of CLI, EL, and LA are plotted in Figure 12. It has been illustrated in section 3.2.1 that the simulated aerosol CONCsur in this study were smaller than observational studies by 1~2 orders of magnitude. Therefore, for calibration, the simulated winter daily aerosol CONCsur over southern China are amplified by 10 times before plotting the frequency distributions.

It is seen from Figure 12 that the frequency distribution of the simulated winter daily aerosol CONCsur over southern China is a little right-skewed in the group of CLI, reaching peak at around 65 μg m^{-3}. The frequency distribution of the simulated winter daily aerosol CONCsur over southern China in the group of LA is a little left-shifting compared with that in CLI when aerosol CONCsur is larger than 40 μg m^{-3}. The frequency distribution of the simulated winter daily aerosol CONCsur over southern China in EL is a little right-shifting compared with that in CLI. The average numbers of days in winter with aerosol CONCsur bellow 40, between 40~80, and above 80 μg m^{-3} in CLI, EL, and LA are also given in the top right corner of Figure 12. It is found that the number of days in winter with aerosol CONCsur between 40~80 μg m^{-3} is the largest in LA and smallest in EL. Whereas, the number of days in winter with aerosol CONCsur above 80 μg m^{-3} is the largest in EL and smallest in LA. Figure 12 indicates that southern China tends to have less clean and heavy but more moderate haze days than normal in La Niña winter. Whereas, in El Niño winter, southern China tends to have more heavy but less clean and moderate haze days than normal. This explains why southern China has less (more) haze days but more (less) atmospheric contents of aerosols than

normal in El Niño (La Niña) winter. It should be noted that here we use regional mean aerosol CONCsur over southern China subjected to the low model spatial resolution, which is the reason why the curves in Figure 12 are close to each other. In the real practice, however, haze days and their severities are judged station by station (e.g., Figure 2), and the thresholds are not necessarily the same with what we use in Figure 12. Therefore, we can get some rough information about the effects of ENSO on the winter haze days over southern China from the shifts of curves in Figure 12, but cannot compared it with observational data directly.

It is depicted in Figure 11 that under the emission level of aerosols for the year 2010, the enhanced (weakened) transports of aerosols from South and Southeast Asia to southern China caused by El Niño (La Niña) is the main reason for the increase (decrease) in the atmospheric contents of aerosols over southern China in El Niño (La Niña) winter. Therefore, it is expected that when the emissions of aerosols over South and Southeast Asia diminish in the future, the contradiction between the influences of ENSO on the winter haze days and atmospheric contents of aerosols over southern China will also disappear.

4 Conclusions and discussions

The effects of ENSO on the winter haze days and atmospheric contents of aerosols over China are discussed statistically and numerically. Statistical results show that southern China tends to have less (more) haze days than normal in El Niño (La Niña) winter, which is in line with the simulated more (less) winter precipitation over southern China caused by El Niño (La Niña). Statistical results indicate that the relationships between the winter haze days over northern and eastern China and ENSO are not significant. Numerical results also reveal that the influences of ENSO on the winter atmospheric contents of aerosols over northern and eastern China are not that obvious as over southern China. As a tropical phenomenon, it seems that ENSO affects the winter haze pollution over southern China more significantly than it does over northern and eastern China.

Numerical results indicate that the atmospheric contents of aerosols over southern China are more (less) than normal in El Niño (La Niña) winter, which is to some extent not in line with the effects of ENSO on the winter haze days of the region. In 2010, South and Southeast Asia have become important source areas of anthropogenic aerosols (Zhang et al., 2016). The enhanced southwesterly (northeasterly) at the northwest of the winter anomalous anticyclone (cyclone) over the Philippine Sea caused by El Niño (La Niña) enhanced (weakened) the transports of aerosols from South and Southeast Asia to southern China.

The frequency distributions of the simulated daily surface concentrations of aerosols in winter over southern China indicate that the region tends to have more heavy (moderate) haze days, but less clean and moderate (heavy) haze days than normal in El Niño (La Niña) winter. But it should be noted again that the emission data of aerosols used in our study are fixed in 2010, and if the emissions of aerosols change the story may be different.

Many studies have found that the haze pollution over northern and eastern China was influenced by the EAWM, as we have cited in section 1. And previous studies also found that ENSO could influence the strength of the EAWM, as we have discussed in section 3.2.2 that El Niño can weaken the EAWM. It is expected that there will be some connection between ENSO and the winter haze pollution over northern and eastern China. However, the connection between ENSO and the winter haze pollution over northern and eastern China is not strong, e.g., the correlations between the winter haze days of the two regions and ENSO are not significant. This makes us to think the way how haze pollutants over the north part of China are cleared away in winter. Usually, a few clean days in the north part of China follow a breakout of a block over high latitude Asia, during which a stream of cold air sweeps southwardly and rapidly from the Siberia or Mongolia. Therefore, we can get some information about the influence of ENSO on the winter haze pollution over the north part of China from the frequency of cold air recorded in China in El Niño and La Niña winters. In the Decembers of 1986 (during the 1986/1987 El Niño event) and 2010 (during the 2010/2011 La Niña event), cold air happened in China both for 7 times, the maximum of the same month during 1960–2011 (Figure 5S). This indicates that El Niño (La Niña) does not necessarily reduce (increase) the cold air frequency of China in winter, even though it can weaken (strengthen) the EAWM. To the contrary, it seems that El Niño (La Niña) is in favor of (not in favor of) the cold air frequency of China in winter (Figure 6S). The relationship between ENSO and the cold air frequency of China in winter makes the connection between ENSO and the winter haze pollution over the north part of China more complicated than it is expected simply from the perspective of the EAWM. The cold air frequency of China in winter is also influenced by the upstream conditions in the Atlantic Ocean, the Arctic ice, and the Eurasian snow cover (not shown). This emphasizes the importance of exploring the comprehensive effects of ENSO and the extratropical systems on the haze pollution of China.

Haze pollution is a very sophisticated problem, because it is the comprehensive result of human activities and weather conditions. Weather conditions determine the dispersions and removals of haze particles over a specific region, influence the

complex chemistry reactions among different components, and also connect the haze pollution of a specific region with the emissions of neighboring regions. To be more complicated, haze pollution and weather conditions interact with each other closely over some areas. This work explores the effects of ENSO on the winter haze pollution over China under relatively simple experimental settings, with prescribed SST and fixed aerosol emissions, which means that SST does not response to aerosols. Besides, the chemistry reactions in the model we used is also simplified, especially without the complex reactions related to nitrate aerosols. Therefore, studies with more sophisticated experimental designs (e.g., with atmosphere and ocean coupled models) and chemistry schemes are still in need in the future as to the topic discussed in this work.

Author contributions. The work was done under the guidance of Hua Zhang. Shuyun Zhao and Hua Zhang designed the experiment, and prepared the manuscript. Bing Xie conducted model simulations. The analysis of results and preparation of all figures and tables were done by Shuyun Zhao.

Acknowledgement

This work was financially supported by the (Key) National Natural Science Foundation of China (91644211&41575002). And we would like to thank Dr. Shao Sun of the National Climate Center, Chinese Meteorological Administration, for his kind help in plotting figures.

References

Bjerknes, J.: Large-scale atmospheric response to the 1964-65 Pacific equatorial warming, J. Phys. Oceanogr., 2, 212–217, doi: 10.1175/1520-0485(1972)002<0212:LSARTT>2.0.CO;2, 1972.

Cao, J.-J., Lee, S.-C., Chow, J.-C., Watson, J. G., Ho, K.-F., Zhang, R.-J., Jin, Z.-D., Shen, Z.-X., Chen, G.-C., Kang, Y.-M., Zou, S.-C., Zhang, L.-Z., Qi, S.-H., Dai, M.-H., Cheng, Y., and Hu, K.: Spatial and seasonal distributions of carbonaceous aerosols over China, J. Geophys. Res., 112, D22S11, doi: 10.1029/2006JD008205, 2007.

Cai, W.-J., Li, K., Liao, H., Wang, H.-J., and Wu, L.-X.: Weather conditions conducive to Beijing severe haze more frequent under climate change, Nature Climate Change, Nat. Clim. Change, 7, 257–262, doi: 10.1038/nclimate3249, 2017.

Chang, C.-P., Zhang, Y.-S., and Li, T.: Interannual and interdecadal variations of the East Asian summer monsoon and tropical Pacific SSTs. Part I: Roles of the subtropical ridge, J. Climate, 13, 4310–4325, doi: 10.1175/1520-

0442(2000)013<4310:IAIVOT>2.0.CO;2, 2000.

Chen, W., Graf, H. F., and Huang, R.-H.: The interannual variability of East Asian winter monsoon and its relation to the summer monsoon, Adv. Atmos. Sci., 17, 48–60, doi: 10.1007/s00376-000-0042-5, 2000.

Chen, W., Lan, X.-Q., Wang, L., and Ma, Y.: The combined effects of the ENSO and the Arctic Oscillation on the winter climate anomalies in East Asia, Chin. Sci. Bull., 58(12), 1355–1362, doi: 10.1007/s11434-012-5654-5, 2013.

Chen, H.-P. and Wang, H.-J.: Haze days in North China and the associated atmospheric circulations based on daily visibility data from 1960 to 2012, J. Geophys. Res.: Atmos., 120 (12), 5895–5909, doi: 10.1002/2015JD023225, 2015.

Chin M.: Dirtier air from a weaker monsoon, Nature Geoscience, 5, 449–450, doi: 10.1038/ngeo1513, 2012.

Dawson, J. P., Adams, P. J., and Pandis, S. N.: Sensitivity of $PM_{2.5}$ to climate in the Eastern US: a modeling case study, Atmos. Chem. Phys., 7, 4295–4309, doi: 10.5194/acp-7-4295-2007, 2007.

Ding, Y.-H. and Liu, Y.-J.: Analysis of long-term variations of fog and haze in China in recent 50 years and their relations with atmospheric humidity, Sci. China Earth Sci., 57, 36–46, doi: 10.1007/s11430-013-4792-1, 2014.

Feng, J., Li, J.-P., Zhu, J.-L., and Liao, H.: Influences of El Nino Modoki event 1994/1995 on aerosol concentrations over southern China, J. Geophys. Res: Atmos., 121(4), 1637–1651, doi: 10.1002/2015JD023659, 2016.

Feng, J., Li, J.-P., Zhu, J.-L., Liao, H., and Yang, Y.: Simulated contrasting influences of two La Niña Modoki events on aerosol concentrations over eastern China, J. Geophys. Res: Atmos., 122, 2734–2749, doi: 10.1002/2016JD026175, 2017.

Gao, H. and Li, X.: Influences of El Nino Southern Oscillation events on haze frequency in eastern China during boreal winters, Int. J. Climatol., 35(9), 2682–2688, doi: 10.1002/joc.4133, 2015.

Gong, S.-L., Barrie, L. A., and Lazare, M.: Canadian Aerosol Module (CAM): a size-segregated simulation of atmospheric aerosol processes for climate and air quality models 2. Global sea-salt aerosol and its budgets, J. Geophys. Res., 107(D24), doi: 10.1029/2001JD002004, 2002.

Gong, S.-L., Barrie, L. A., Blanchet, J.-P., von Salzen, K., Lohmann, U., Lesins, G., Spacek, L., Zhang, L.-M., Girard, E., Lin, H., Leaitch, R., Leighton, H., Chylek, P., and Huang, P.: Canadian aerosol module: A size-segregated simulation of atmospheric aerosol processes for climate and air quality models 1. Module development, J. Geophys. Res., 108(D1), doi: 10.1029/2001JD002002, 2003.

He, S.-P. and Wang, H.-J.: Oscillating relationship between the East Asia winter monsoon and ENSO, J. Climate, 26, 9819–9838, doi: 10.1175/JCLI-D-13-00174.1, 2013.

Huang, R.-H. and Wu, Y.-F.: The influence of ENSO on the summer climate change in China and its mechanism, Adv. Atmos. Sci., 6 (1), 21–32, doi: 10.1007/BF02656915, 1989.

Huang, R.-H., Chen, J.-L., Wang, L., and Lin, Z.-D.: Characteristics, processes, and causes of the spatio-temporal variabilities of the East Asian monsoon system, Adv. Atmos. Sci., 29, 910–942, doi: 10.1007/s00376-012-2015-x, 2012.

Hurrell, J. W., Hack, J. J., Shea, D., Caron, J. M., and Rosinski, J.: A new sea surface temperature and sea ice boundary data set for the Community Atmosphere Model, J. Climate, 21, 5145–5153, doi: 10.1175/2008JCLI2292.1, 2008.

Jacob, D. J. and Winner, D. A.: Effects of climate change on air quality, Atmos. Environ., 43, 51–63, doi: 10.1016/j.atmosenv.2008.09.051, 2009.

Kang, D., and Lee, M.-I.: ENSO influence on the dynamical seasonal prediction of the East Asian Winter Monsoon, Clim. Dyn., doi: 10.1007/s00382-017-3574-4, 2017.

Kim, J.-W., An, S.-I., Jun, S.-Y., Park, H.-J., and Yeh, S.-W.: ENSO and East Asian winter monsoon relationship modulation associated with the anomalous northwest Pacific anticyclone, Clim. Dyn., doi: 10.1007/s00382-016-3371-5, 2016.

Lau, N.-C. and Nath, M. J.: Atmosphere-ocean variations in the Indo-Pacific sector during ENSO episodes, J. Climate, 16, 3–20, doi: 10.1175/1520-0442(2003)016<0003:AOVITI>2.0.CO;2, 2003.

Li, Q., Zhang, R.-H., and Wang, Y.: Interannual variation of the wintertime fog-haze days across central and eastern China and its relation with East Asian winter monsoon, Int. J. Climatol., 36, 346–354, doi: 10.1002/joc.4350, 2016a.

Li, Y., Lu, R.-Y., and Dong, B.-W.: The ENSO-Asian monsoon interaction in a coupled ocean-atmosphere GCM, J. Climate, 20, 5164–5177, doi: 10.1175/JCLI4289.1, 2007.

Li, Y., and Yang, S.: A dynamical index for the East Asian winter monsoon, J. Climate, 23(15), 4255–4262, doi: 10.1175/2010JCLI3375.1, 2010.

Li, Z.-Q., Lau, W. K.-M., Ramanathan, V., Wu, G., Ding, Y., Manoj, M.-G., Liu, J., Qian, Y., Li, J., Zhou, T., Fan, J., Rosenfeld, D., Ming, Y., Wang, Y., Huang, J., Wang, B., Xu, X., Lee, S.-S., Cribb, M., Zhang, F., Yang, X., Zhao, C., Takemura, T., Wang, K., Xia, X., Yin, Y., Zhang, H., Guo, J., Zhai, P.-M., Sugimoto, N., Babu, S.-S., and Brasseur G.-P.: Aerosol and monsoon

climate interactions over Asia, Rew. Geophys., 54, 866–929, doi: 10.1002/2015RG000500, 2016b.

Liu, X.-D., Yan, L.-B., Yang, P., Yin, Z.-Y., and North, G. R.: Influence of Indian summer monsoon on aerosol loading in East Asia, J. Appl. Meteor. Climatol., 50, 523–533, doi: 10.1175/2010JAMC2414.1, 2011.

Mu, M. and Zhang, R.-H.: Addressing the issue of fog and haze: A promising perspective from meteorological science and technology, Sci. China Earth Sci., 57, 1–2, doi: 10.1007/s11430-013-4791-2, 2014.

Rasmusson, E. M. and Carpenter, T. H.: Variations in tropical sea surface temperature and surface wind fields associated with the Southern Oscillation/El Niño, Mon. Wea. Rev., 110, 354–384, doi: 10.1175/1520-0493(1982)110<0354:VITSST>2.0.CO;2, 1982.

Tao, M.-H., Chen, L.-F., Xiong, X.-Z., Zhang, M.-G., Ma, P.-F., Tao, J.-H., and Wang, Z.-F.: Formation process of the widespread extreme haze pollution over northern China in January 2013: Implications for regional air quality and climate, Atmos. Environ., 98, 417–425, doi: 10.1016/j.atmosenv.2014.09.026, 2014.

Tao, M.-H., Chen, L.-F., Wang, Z.-F., Wang, J., Tao, J.-H., and Wang, X.-H.: Did the widespread haze pollution over China increase during the last decade? A satellite view from space, Environ. Res. Lett., 11(5),054019, doi: 10.1088/1748-9326/11/5/054019, 2016.

Wang, B., Wu, R.-G., and Fu, X.-H.: Pacific-East Asian Teleconnection: How does ENSO affect East Asian Climate? J. Climate, 13, 1517–1536, doi: 10.1175/1520-0442(2000)013<1517:PEATHD>2.0.CO;2, 2000.

Wang, H.-J., Chen, H.-P., and Liu, J.-P.: Arctic sea ice decline intensified haze pollution in eastern China, Atmos., Oceanic Sci. Lett., 8, 1–9, doi: 10.3878/AOSL20140081, 2015.

Wang. L. and Chen, W.: An intensity index for the East Asian winter monsoon, J. Climate, 27, 2361–2374, doi: 10.1175/JCLI-D-13-00086.1, 2014.

Wang, Y.-S., Yao, L., Wang, L.-L., Liu, Z.-R., Ji, D.-S., Tang, G.-Q., Zhang, J.-K., Sun, Y., Hu, B., and Xin, J.-Y.: Mechanism for the formation of the January 2013 heavy haze pollution episode over central and eastern China, Sci. China Earth Sci., 57, 14–25, doi: 10.1007/s11430-013-4773-4, 2014a.

Wang, Z.-F., Li, J., Wang, Z., Yang, W.-Y., Tang, X., Ge, B.-Z., Yan, P.-Z., Zhu, L.-L., Chen, X.-S., Chen, H.-S., Wand, W., Li, J.-J., Liu, B., Wang, X.-Y., Wand, W., Zhao, Y.-L., Lu, N., and Su, D.-B.: Modeling study of regional severe hazes over mid-

eastern China in January 2013 and its implications on pollution prevention and control, Sci. China Earth Sci., 57, 3–13, doi: 10.1007/s11430-013-4793-0, 2014b.

Wang, Z.-L., Zhang, H., and Zhang, X.-Y.: Projected responses of East Asian summer monsoon system to future reductions in emissions of anthropogenic aerosols and their precursors, Clim. Dyn., 47(5), 1455–1468, doi: 10.1007/s00382-015-2912-7, 2015.

Wu, T.-W., Yu, R.-C., Zhang, F., Wang, Z.-Z., Dong, M., Wang, L.-N., Jin, X., Chen, D.-L., and Li, L.: The Beijing Climate Center atmospheric general circulation model: description and its performance for the present-day climate, Clim. Dyn., 34, 123–147, doi: 10.1007/s00382-008-0487-2, 2010.

Wu, R.-G., Wen, Z.-P., and He, Z.-Q.: ENSO contribution to aerosol variations over the Maritime Continent and the Western North Pacific during 2000–10, J. Climate, 26, 6541–6560, doi: 10.1175/JCLI-D-12-00253.1, 2013

Yan, L.-P., Liu, X.-D., Yang, P., Yin, Z.-Y., and North, G. R.: Study of the impact of summer monsoon circulation on spatial distribution of aerosols in East Asia based on numerical simulation, J. Appl. Meteor. Climatol., 50, 2270–2282, doi: 10.1175/2011JAMC-D-11-06.1, 2011.

Yang, Y., Liao, H., and Li, J.: Impacts of the East Asian summer monsoon on interannual variations of summertime surface-layer ozone concentrations over China, Atmos. Chem. Phys., 14, 6867–6880, doi: 10.5194/acp-14-6867-2014, 2014.

Zhai, P.-M., Yu, R., Guo, Y.-J., Li, Q.-X., Ren, X.-J., Wang, Y.-Q., Xu, W.-H., Liu, Y.-J., and Ding, Y.-H.: The strong El Niño of 2015/16 and its dominant impacts on global and China's climate, J. Meteor. Res., 30(3), 283–297, doi: 10.1007/s13351-016-6101-3, 2016.

Zhang, H., Wang, Z.-L., Wang, Z.-Z., Liu, Q.-X., Gong, S.-L., Zhang, X.-Y., Shen, Z.-P., Lu, P., Wei, X.-D., Che, H.-Z., and Li, L.: Simulation of direct radiative forcing of aerosols and their effects on East Asia climate using an interactive AGCM-aerosol coupled system, Clim. Dyn., 38, 1675–1693, doi: 10.1007/s00382-011-1131-0, 2012.

Zhang, H., Zhao, S.-Y., Wang, Z.-L., Zhang, X.-Y., and Song, L.-C.: The updated effective radiative forcing of major anthropogenic aerosols and their effects on global climate at present and in the future, Int. J. Climatol., 36(12), 4029–4044, doi: 10.1002/joc.4613, 2016.

Zhang, L., Liao, H., and Li, J.-P.: Impacts of Asian summer monsoon on seasonal and interannual variations of aerosols over

eastern China, J. Geophys. Res., 115, D716, doi: 10.1029/2009JD012299, 2010.

Zhang, R.-H., Sumi, A., and Kimoto, M.: A diagnostic study of the impact of El Niño on the precipitation in China, Adv. Atmos. Sci., 16(2), 229–241, doi: 10.1007/BF02973084, 1999.

Zhang, R.-H., Li, Q., and Zhang, R.-N.: Meteorological conditions for the persistent severe fog and haze event over eastern China in January 2013, Sci. China Earth Sci., 57, 26–35, doi: 10.1007/s11430-013-4774-3, 2014.

Zhang, X.-Y., Wang, Y.-Q., Niu, T., Zhang, X.-C., Gong, S.-L., Zhang, Y.-M., and Sun, J.-Y.: Atmospheric aerosol compositions in China: spatial/temporal variability, chemical signature, regional haze distribution and comparisons with global aerosols, Atmos. Chem. Phys., 12, 779–799, doi: 10.5194/acp-12-779-2012, 2012.

Zhang, Y.-L. and Cao, F.: Fine particulate matter ($PM_{2.5}$) in China at a city level, Scientific Reports, 5, 14884, doi: 10.1038/srep14884, 2015.

Zhao, S.-Y., Zhi, X.-F., Zhang, H., Wang, Z.-L., and Wang, Z.-Z.: Primary assessment of the simulated climatic state using a coupled aerosol-climate model BCC_AGCM2.0.1_CAM. Climatic and Environmental Research (in Chinese), 19(3), 265–277, doi: 10.3878/j.issn.1006-9585.2012.12015, 2014.

Zhao, S.-Y., Chen, L.-J., and Cui, T.: Effects of ENSO phase-switching on rainy-season precipitation in north China, Chinese Journal of Atmospheric Sciences (in Chinese), doi: 10.3878/j.issn.1006-9895.1701.16226, 2017.

Zhu, J.-L., Liao, H., and Li J.-P.: Increases in aerosol concentrations over eastern China due to the decadal-scale weakening of the East Asian summer monsoon, Geophys. Res. Lett., 39, L09809, doi: 10.1029/2012GL051428, 2012.

Zou, Y.-F., Wang, Y.-H., Zhang, Y.-Z., and Koo, J.-H.: Arctic sea ice, Eurasia snow, and extreme winter haze in China, Sci. Adv., 3, e1602751, doi: 10.1126/sciadv.1602751, 2017.

Tables and Figures

Table 1. Simulation set-up.

Group name	SST	Running time	Output frequency
CLI	Climatologic SST	Oct.^{0}–Aug.^{1}	Monthly & Daily
EL	Climatologic SST + $\Delta SST_{El\ Niño}$	Oct.^{0}–Feb.^{1}	Monthly & Daily

LA	Climatologic SST + $\Delta SST_{La\ Niña}$	Oct.^{0}–Feb.^{1}	Monthly & Daily

The superscripts of the 3rd column: 0 and 1 represent the 1st and 2nd model year, respectively.

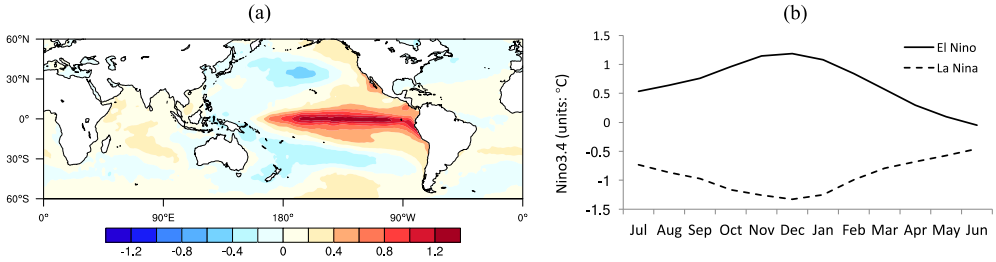

Figure 1. (a) Typical ENSO mode (units: °C/°C) and (b) average monthly Niño3.4 (units: °C) of 21 El Niño and 18 La Niña events from 1951 to 2015.

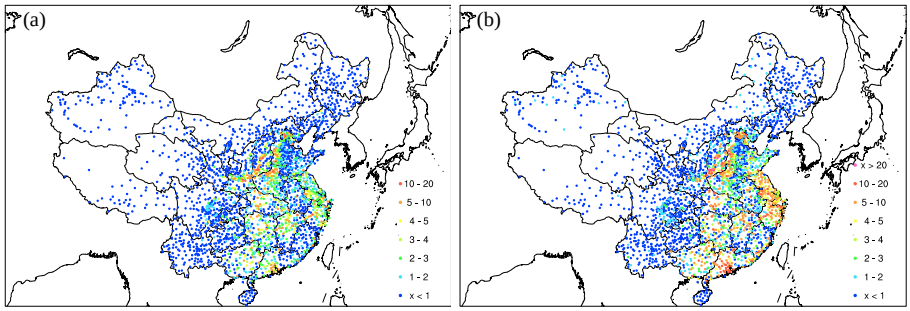

Figure 2. The winter-average monthly haze days (units: days/month) during the years of (a) 1960-2013 and (b) 2000-2013 over main land China.

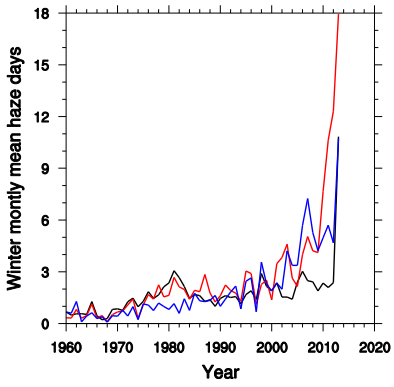

Figure 3. Time series of the winter-average monthly haze days (units: days/month) of JJJ (black), JZH (red), and GG (blue).

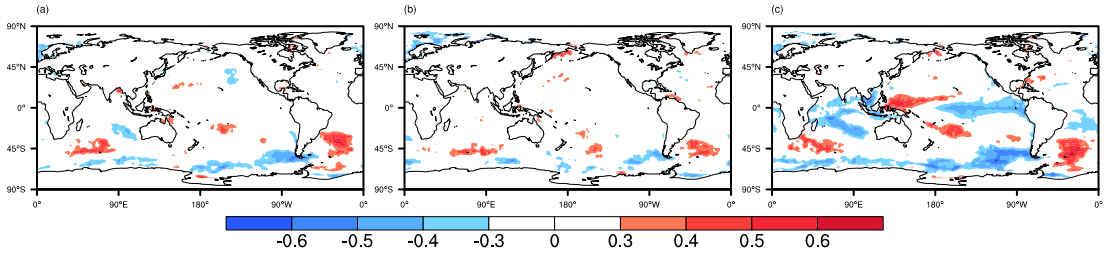

Figure 4. Correlation coefficients (unitless) of the monthly haze days of (a) JJJ, (b) JZH, and (c) GG with SST in winter, after applying a band-pass filtering of 2-8 years to both the data of haze days and SST. Shade denotes that results pass 95% significance level.

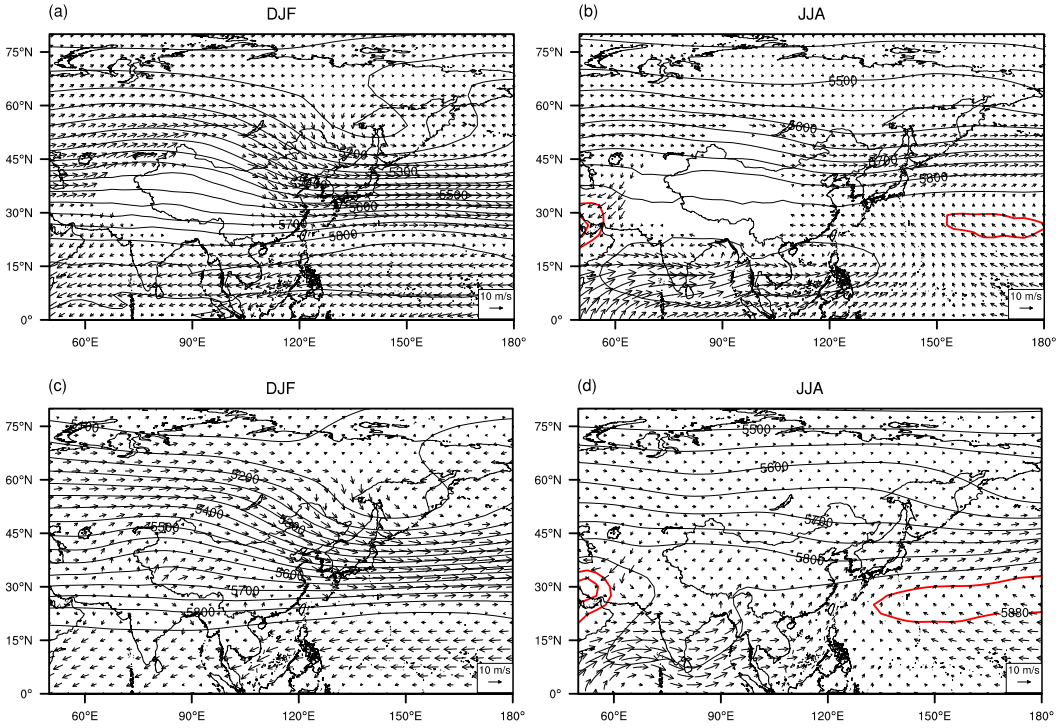

Figure 5. Comparisons between (a–b) the simulated and (c–d) reanalysis winter and summer geopotential height at 500 hPa (contour, units: gpm) and wind at 850 hPa (vector, units: m s^{-1}), with the blank places in (a) and (b) are because of the influence of the Tibetan Plateau. Model results are from the group of CLI, and reanalysis data are from NCEP.

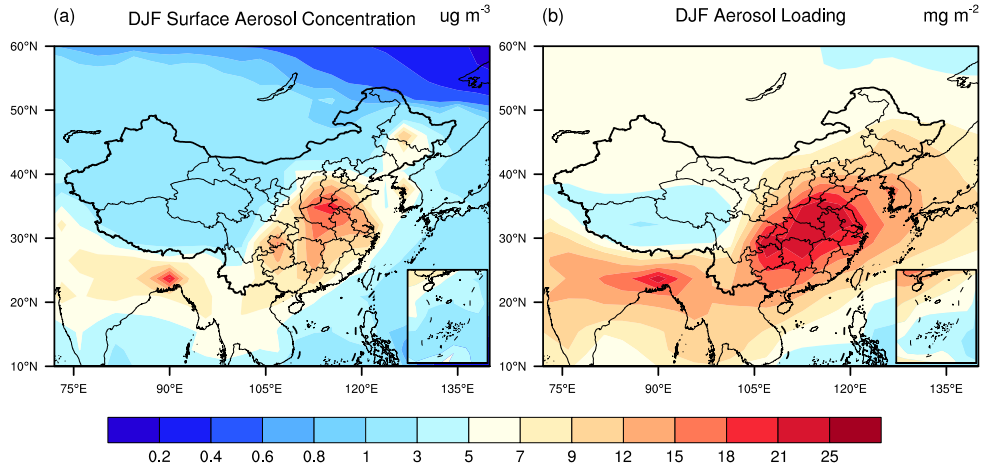

Figure 6. The simulated winter-average (a) surface aerosol concentrations (units: μg m^{-3}) and (b) aerosol loadings (units: mg m^{-2}) in

the group of CLI.

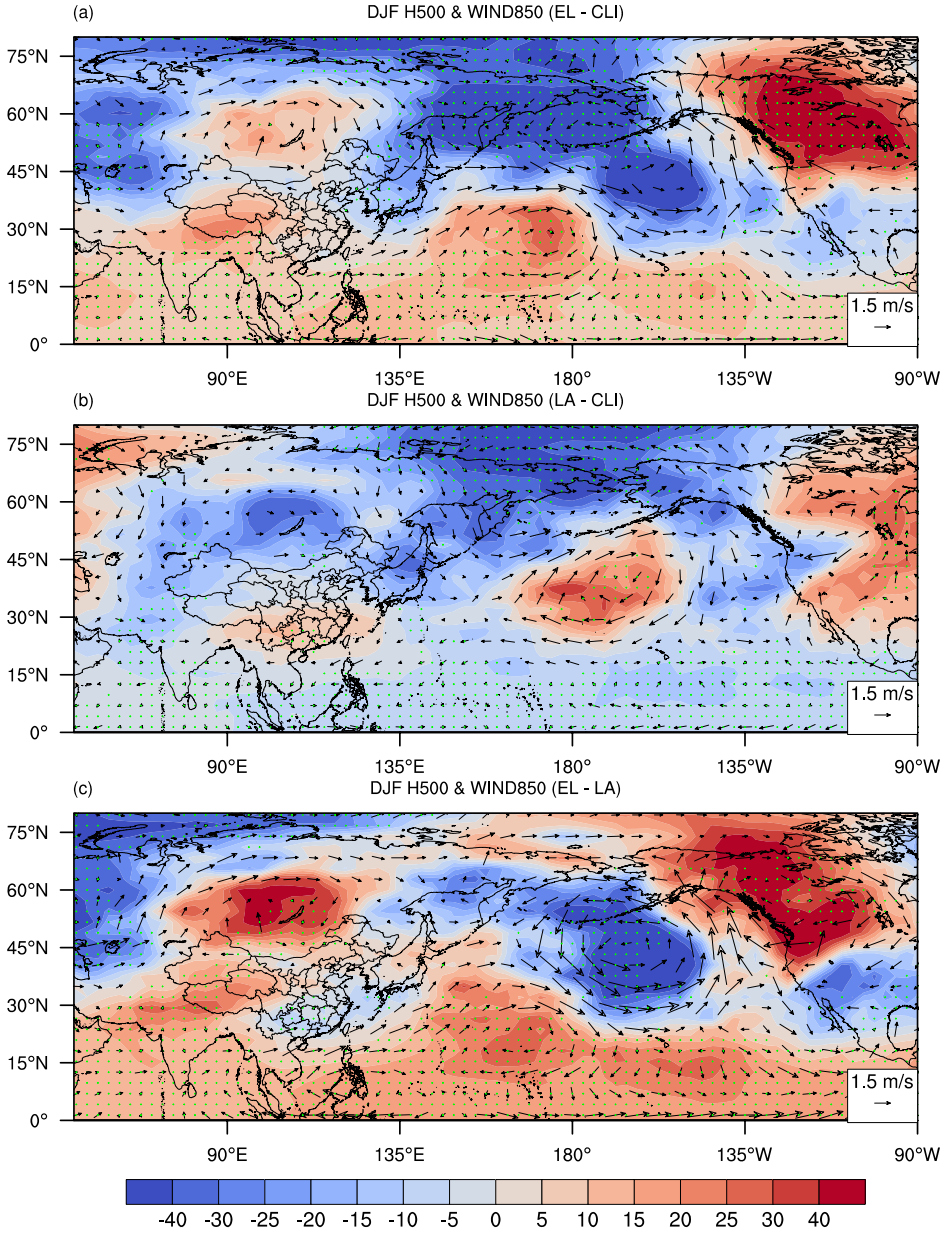

Figure 7. Medians of the simulated differences in winter-average geopotential height at 500 hPa (H500, shaded, units: gpm) and wind at 850 hPa (WIND850, vector, units: m s^{-1}) between (a) EL and CLI, (b) LA and CLI, and (c) EL and LA, with green dots indicating that the differences of H500 between more than 70% pairs of ensemble members have the same sign with the median

differences.

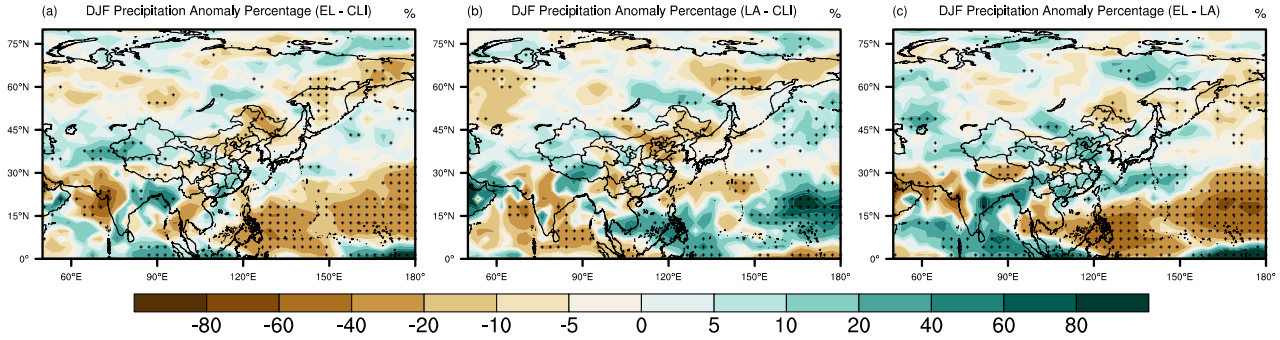

Figure 8. Medians of the simulated differences in winter-average precipitation in percentage (units: %) between (a) EL and CLI, (b) LA and CLI, and (c) EL and LA, with black dots indicating that the differences between more than 70% pairs of ensemble members have the same sign with the median differences.

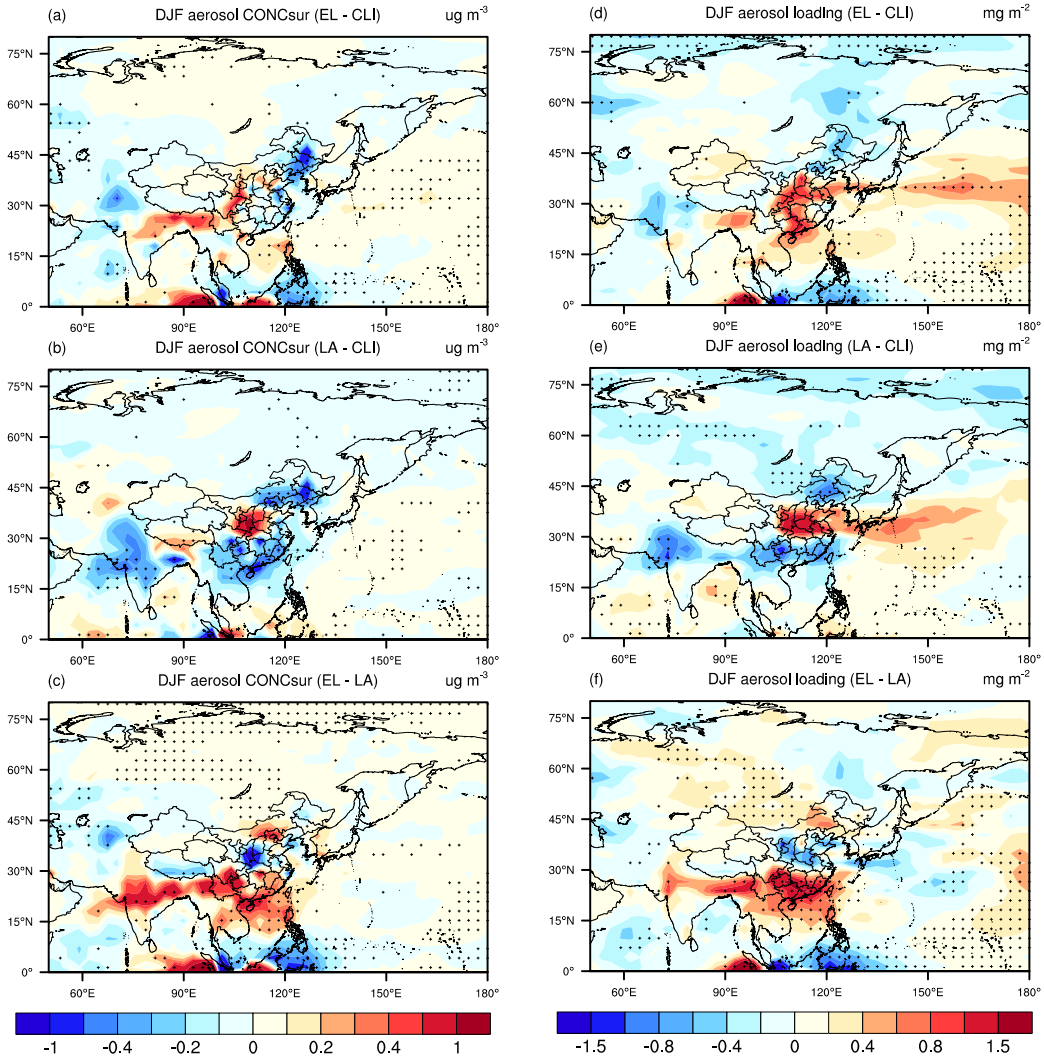

Figure 9. Medians of the simulated differences in winter-average aerosol surface concentrations (left panel, units: μg m^{-3}) and aerosol loadings (right panel, units: mg m^{-2}) between (a)~(d) EL and CLI, (b)~(e) LA and CLI, and (c)~(f) EL and LA, with black dots indicating that the differences between more than 70% pairs of ensemble members have the same sign with the median differences.

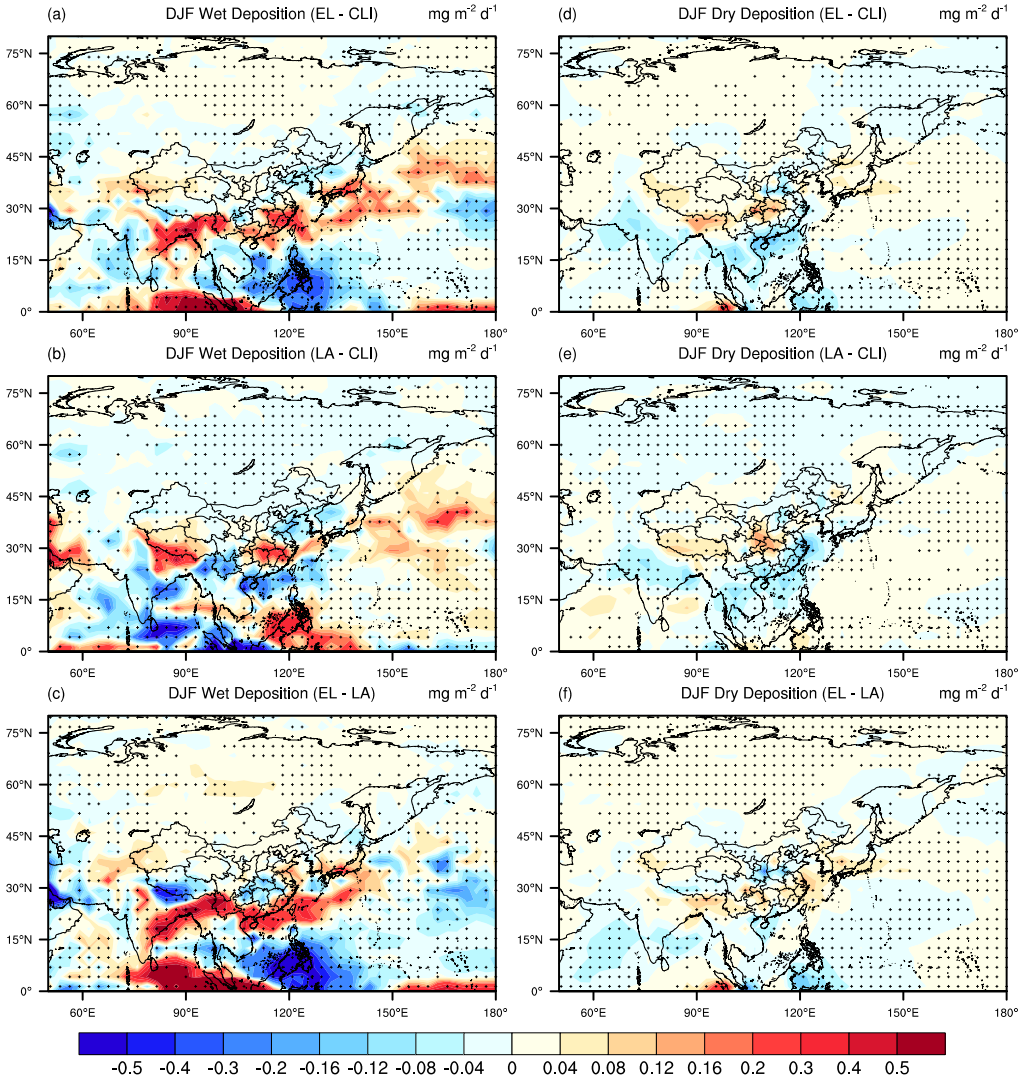

Figure 10. Medians of the simulated differences in winter-average wet depositions (left panel) and dry depositions (right panel) of aerosols (units: mg m^{-2} d^{-1}) between (a)~(d) EL and CLI, (b)~(e) LA and CLI, and (c)~(f) EL and LA, with black dots indicating that the differences between more than 70% pairs of ensemble members have the same sign with the median differences.

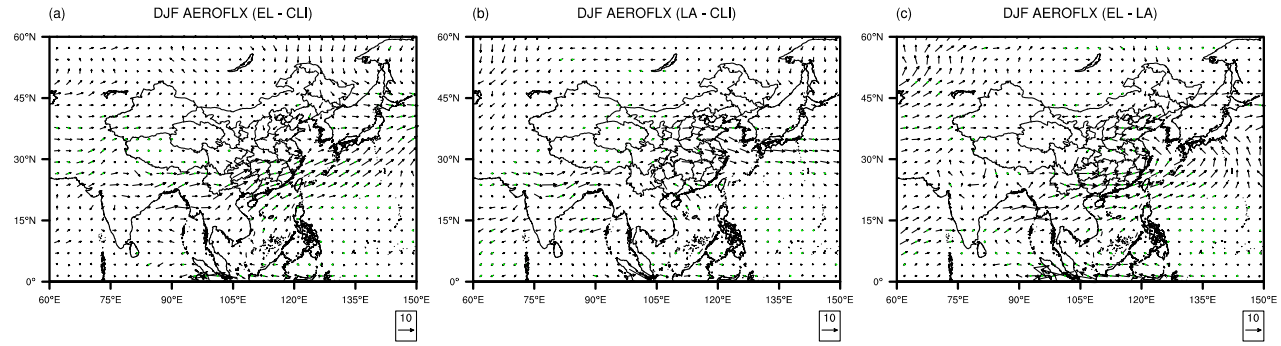

Figure 11. Medians of the simulated differences in the winter-average vertical integral of aerosol horizontal fluxes (AEROFLX, units: kg m^{-1} s^{-1}) between (a) EL and CLI, (b) LA and CLI, and (c) EL and LA, with green dots indicating that the differences of the zonal components of AEROFLX between more than 70% pairs of ensemble members have the same sign with the median differences.

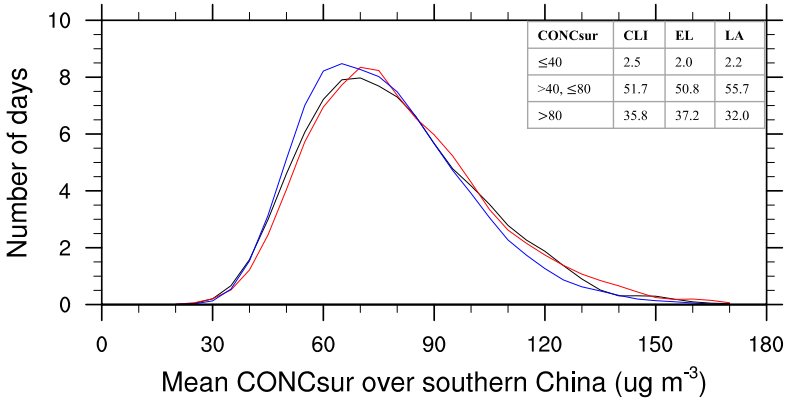

Figure 12. Frequency distributions of the simulated winter daily surface aerosol concentrations (CONCsur, units: μg m^{-3}) averaged over southern China (after being amplified by 10 times), with black, red and blue lines representing the results from CLI, EL, and LA, respectively; The average numbers of days in winter with CONCsur ≤ 40, 40 <CONCsur ≤ 80, and CONCsur>80 in CLI, EL, and LA are given in the table at the top right corner.